Title

A myelin basic protein fragment induces sexually dimorphic transcriptome signatures of neuropathic pain in mice

Journal

Journal of Biological Chemistry, 295(31)

ISSN

0021-9258

Authors

Chernov, Andrei V

Hullugundi, Swathi K

Eddinger, Kelly A

et al.

Publication Date

2020-07-01

DOI

10.1074/jbc.ra120.013696

A myelin basic protein fragment induces sexually dimorphic transcriptome signatures of neuropathic pain in mice

Received for publication, March 31, 2020, and in revised form, June 11, 2020 Published, Papers in Press, June 12, 2020, DOI 10.1074/jbc.RA120.013696

Andrei V. Chernov[1,2,*], Swathi K. Hullugundi[1,3], Kelly A. Eddinger[1], Jennifer Dolkas[1,3], Albert G. Remacle[2], Mila Angert[1,3], Brian P. James[2], Tony L. Yaksh[1], Alex Y. Strongin[2], and Veronica I. Shubayev[1,3,*]

From the [1]Department of Anesthesiology, University of California, San Diego, La Jolla, California, USA, the [2]Infectious and Inflammatory Disease Center, Sanford Burnham Prebys Medical Discovery Institute, La Jolla, California, USA, and the [3]Veterans Affairs San Diego Healthcare System, La Jolla, California, USA

Edited by Roger J. Colbran

In the peripheral nerve, mechanosensitive axons are insulated by myelin, a multilamellar membrane formed by Schwann cells. Here, we offer first evidence that a myelin degradation product induces mechanical hypersensitivity and global transcriptomics changes in a sex-specific manner. Focusing on downstream signaling events of the functionally active 84-104 myelin basic protein (MBP(84-104)) fragment released after nerve injury, we demonstrate that exposing the sciatic nerve to MBP(84-104) via endoneurial injection produces robust mechanical hypersensitivity in female, but not in male, mice. RNA-seq and systems biology analysis revealed a striking sexual dimorphism in molecular signatures of the dorsal root ganglia (DRG) and spinal cord response, not observed at the nerve injection site. Mechanistically, intra-sciatic MBP(84-104) induced phospholipase C (PLC)-driven (females) and phosphoinositide 3-kinase-driven (males) phospholipid metabolism (tier 1). PLC/inositol trisphosphate receptor (IP3R) and estrogen receptor co-regulation in spinal cord yielded Ca^{2+}-dependent nociceptive signaling induction in females that was suppressed in males (tier 2). IP3R inactivation by intrathecal xestospongin C attenuated the female-specific hypersensitivity induced by MBP(84-104). According to sustained sensitization in tiers 1 and 2, T cell–related signaling spreads to the DRG and spinal cord in females, but remains localized to the sciatic nerve in males (tier 3). These results are consistent with our previous finding that MBP(84-104)–induced pain is T cell–dependent. In summary, an autoantigenic peptide endogenously released in nerve injury triggers multisite, sex-specific transcriptome changes, leading to neuropathic pain only in female mice. MBP(84-104) acts through sustained co-activation of metabolic, estrogen receptor–mediated nociceptive, and autoimmune signaling programs.

Chronic pain is a major public health problem worldwide (1–3). Development of universal analgesic therapies has failed partly due to sex-related differences in pain prevalence, incidence, mechanisms, and drug efficacy (4–9). Recent evidence has started to emerge that immune response mechanisms to noxious stimuli is sex-specific (8–14). Focal peripheral nerve injury produces pain in response to innocuous tactile stimulation (mechano-allodynia) in part through the activity of hematogenous T cells recruited from systemic circulation (15–18). Seminal research implicated T cell activity in selective mediation of mechano-allodynia in female, but not male, mice with peripheral nerve trauma, as males employed innate immune spinal microglia activity (11, 19). The mechanisms and the specific T cell epitopes released that underlie the female-specific T cell activity in mechano-allodynia remain obscure.

Mechanosensory dorsal root ganglia (DRG) neurons of the leg (sciatic nerve) are among the longest cells in the body, spanning from foot to spine. Their lipid-rich, multilamellar myelin membrane sheath provides electrical and metabolic insulation and ensures fast, saltatory conduction of a tactile-stimulated impulse (20). In healthy nerves, myelin compaction and integrity are maintained via interactions of the intrinsically unstructured, cationic myelin basic protein (MBP) with the anionic membrane phospholipids (21, 22), including phosphatidylinositol 4,5-bisphosphate (PIP2) (23). Disruption of structural and molecular integrity of myelin by peripheral nerve trauma contributes to mechano-allodynia (24–26).

MBP is a putative autoantigen implicated in the pathogenesis of autoimmune demyelinating states of the central (21, 22) and peripheral (27) nervous systems. In female rats with peripheral nerve trauma, we have shown that inhibition of matrix metalloproteinase-mediated proteolysis of MBP attenuates mechano-allodynia at least in part by blocking the release of T cell epitopes of MBP and T cell homing into the nerve (26, 28, 29). Specifically, focal nerve trauma causes release of the immunodominant T cell epitope of MBP comprising the evolutionarily conserved, invariant α-helix ^{87}VVHFF^{91} motif (26, 28–31). To elucidate the downstream events of the MBP peptide exposure in mechano-allodynia, we identified the 84-104 fragment of MBP (MBP(84-104)) as the potent pro-algesic peptide in female rats (29).

In female rats, endoneurial delivery of the pure MBP(84-104), but not the control scramble, peptide by an adjuvant-free injection into an intact sciatic nerve (IS) induces persistent (2 weeks) mechano-allodynia (29, 30, 32). The MBP(84-104)-induced mechano-allodynia in females is refractory to systemically delivered analgesics, such as ketorolac and lidocaine (32). The IS MBP(84-104) mechano-allodynia is T cell-dependent, as shown using athymic nude female rats lacking mature T cells (29) and by mutagenesis of the T cell-binding site of the peptide (30). In contrast to a focal nerve trauma, IS MBP(84-104) is not accompanied by major neuropathological changes (29, 30), making it an attractive model to study sustained mechano-

* For correspondence: Andrei Chernov, achernov@ucsd.edu; Veronica Shubayev, vshubayev@ucsd.edu.

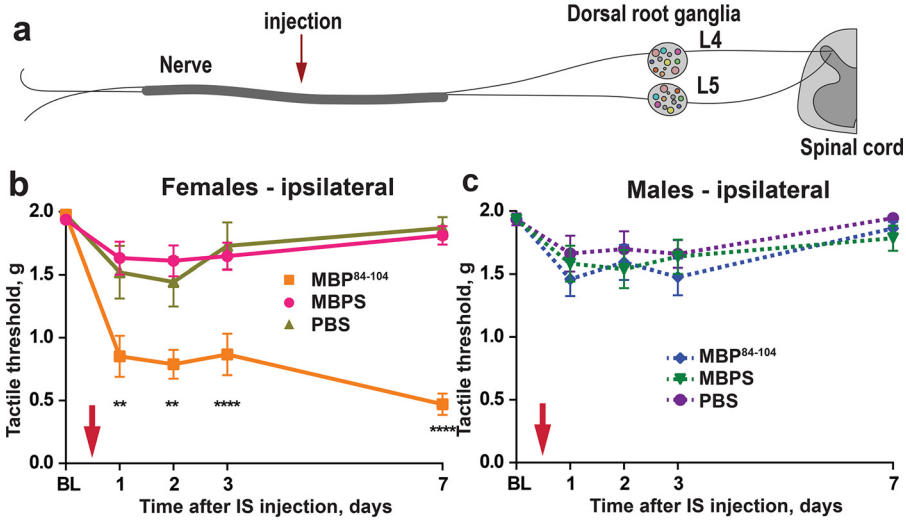

Figure 1. Sexually dimorphic (female-specific) mechano-allodynia induced by IS MBP(84-104). *a,* a schematic diagram of the sciatic nerve (SN), lumbar (L) 4 and L5 DRG, and DSC ipsilateral to intrasciatic (IS) injections. *b* and *c*, von Frey testing of ipsilateral paws in female (*b*) and male (*c*) mice at 1, 2, 3, and 7 days after IS MBP(84-104) ($n = 16$ female, $n = 21$ male) or scramble (MBPS, $n = 21$ female, $n = 15$ male) peptides (30 μg in 3 μl, each), or PBS (3 μl, $n = 8$ female, $n = 14$ male). The mean withdrawal tactile thresholds are in gram force (g) $\pm$ S.E.; two-way ANOVA (*b,* treatment $\times$ time $f = 7.556$ $p \leq 0.0001$, time $f = 17.19$, $p \leq 0.0001$, treatment $f = 33.52$ $p \leq 0.0001$, subject $f = 2.395$, $p \leq 0.0001$; *c,* treatment $\times$ time $f = 0.3755$, $p = 0.9326$, time $f = 7.885$ $p \leq 0.0001$, treatment $f = 0.7275$, $p = 0.4885$, subject $f = 2.015$ $p = 0.0005$) with Dunnett's post hoc test: **, $p \leq 0.01$; ****, $p \leq 0.0001$ relative to the PBS control. *Red arrows* indicate time of IN injection.

allodynia, without background effects of acute degenerative and reparative processes caused by nerve trauma. Based on these data obtained in female rats, we have proposed that the autoimmune pathogenesis of mechano-allodynia arises due to MBP(84-104)/T cell-mediated targeting of myelinated afferents (28–35).

To determine the role of MBP(84-104) as an epitope initiating the sexual dimorphism (female specificity) of T cell action in mechano-allodynia in mice (11), we here comparatively assessed mechanical sensitivity after IS MBP(84-104) in female and male mice. Our comprehensive, comparative, genome-wide transcriptomic analysis revealed molecular signatures in the injected nerve and ipsilateral DRG and spinal cord, with biological processes and signaling cascades under MBP(84-104) control. The present data provide the first evidence that nerve MBP(84-104) exposure is sufficient to induce mechano-allodynia in a sexually dimorphic (female-specific) manner. We here reveal an overarching 3-tier signaling program associated with sex-specific pain mediation and establish a comprehensive, open-access database for future data mining of the mechanisms leading to autoimmune mediation of neuropathic pain, specifically in females.

Results

IS MBP(84-104) triggers female-specific allodynia

Release of MBP(84-104) drives T cell-dependent mechano-allodynia after focal nerve injury in female rodents (29, 30, 32). Whether a comparable process exists in male rodents is not known. The recent evidence of female-specific T cell mediation of mechano-allodynia signaling in C57BL6 mice (11, 19) prompted us to test the algesic effect of MBP(84-104) in female *versus* male C57BL6 mice. Withdrawal thresholds to mechanical stimulation by von Frey filaments were measured in mice that received a single adjuvant-free IS bolus injection of pure MBP(84-104) or scramble (MBPS) peptides, both diluted in PBS (30 μg in 3 μl, each, Fig. 1*a*). PBS vehicle injections (3 μl) served as control.

In agreement with our prior reports in female rats (29, 30, 32), female mice displayed a highly significant reduction in the mechanical force required to evoke hind paw withdrawal (*i.e.* mechano-allodynia) after IS MBP(84-104), but not PBS or MBPS. The allodynia persisted over the 7-day testing period (Fig. 1*b*). In contrast, male mice after IS MBP(84-104) exhibited mechanical thresholds comparable with control MBPS and PBS injection over the 7-day assessment (Fig. 1*c*). No delayed mechanical sensitivity was observed in males over additional testing out to 24 days (data not shown). No hypersensitivity was observed in contralateral paws in either sex (data not shown). We conclude that MBP(84-104) mediates mechano-allodynia selectively in female, but not male, mice.

Sexual dimorphism in global transcriptional program in DRG and spinal cord, not nerve

Global genome-wide expression profiling is used to elucidate precise molecular signatures of pain (12, 29, 32, 36–41). To identify sexually dimorphic mechanisms induced by nerve MBP(84-104) exposure, we harvested ipsilateral sciatic nerve (SN, injection site), DRG, and dorsal spinal cord (DSC, quartered, Fig. 2*a*) tissues from female and male mice at day 7 after IS MBP(84-104), MBPS or PBS, and von Frey testing. Total RNAs were isolated and analyzed by high-throughput cDNA sequencing (RNA-seq).

Based on our extensive behavioral, histological, and molecular, including transcriptomic (GEO ID GSE34868), findings in naive, post-IS PBS, MBPS, MBP(84-104), and other MBP peptide, both ipsilateral and contralateral to injection (28–30, 32, 37), as well as sham-operated and post-nerve injury rodents (37, 42), IS PBS was selected as control for

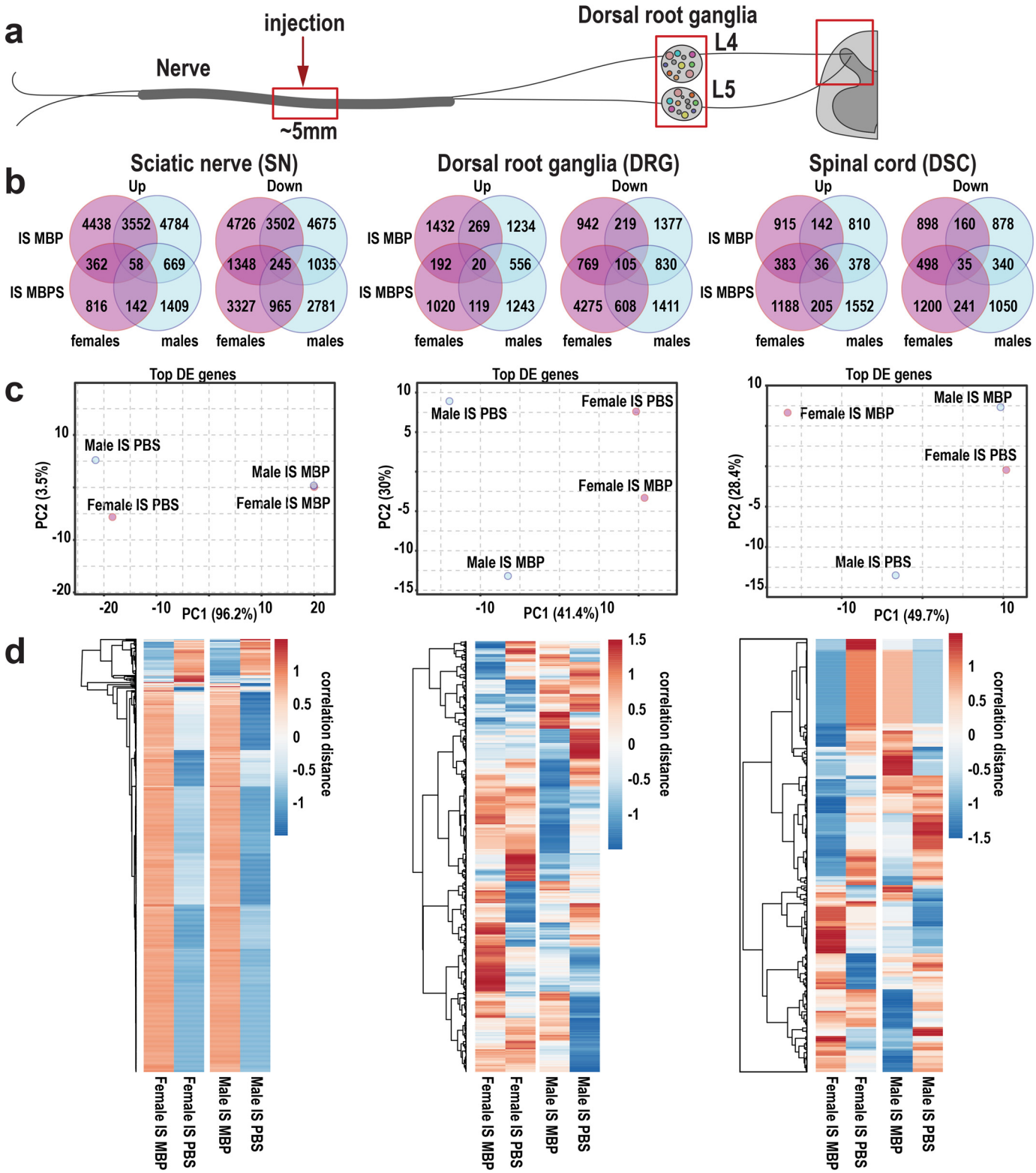

Figure 2. Global transcriptional changes in female and male mice after IS MBP(84-104). *a,* schematic diagram of the sites of transcriptome analysis (*red boxes*): the sciatic nerve ($n = 12$), ipsilateral L4/L5 ($n = 6$) DRG, and L1-6 (quartered, $n = 6$) DSC ipsilateral to IS injection. *b,* Venn diagrams of total DE (relative to IS PBS) gene number increasing (*up*) or decreasing (*down*) in male (*light blue circles*) and female (*purple circles*) SN, DRG, and DSC after IS MBP(84-104) or IS MPBS. The *intersections of circles* represent DE genes similarly changed. DE genes were defined by TPM increase or decrease ($\log_2FC \geq 1$) in IS MBP(84-104) relative to IS PBS. *c,* principal component (*PC*) analysis of the top DE genes in SN, DRG, and DSC, respectively. *Light blue* and *purple circles* indicate males and females, respectively. *d,* hierarchical clustering analysis of the top 1000 up- or down-regulated genes in SN, DRG, and DSC. Genes regulated in IS MBP(84-104), but not IS MBPS were considered. DE genes were clustered based on their respective absolute expression ($\log_2TPM$). Heat map colors indicate correlation distance from low (*blue*) to high (*red*) according to the scale.

assessing sexually dimorphic changes induced by IS MBP (84-104) (algesic) relative to MBPS (not algesic), each solubilized in PBS. We note that physical nerve injury due to injection, represented in the IS PBS group of both female and male tissues, is not a source of sexual dimorphism in pain behavior or transcriptomics response.

Normalized gene expression was computed as transcripts per kilobase of transcript/million mapped reads (TPM). Transcripts with low expression (TPM < 0.05) across 18 samples were excluded from further analysis. A total of 21,900 protein coding genes were identified and further considered for bioinformatic analysis (Fig. 2*b*). Differentially expressed (DE) protein-coding genes with fold-change (FC) ≥ 2 ($\log_2 FC \geq 1$, $p \leq 0.05$) of TPM counts were grouped in MBP(84-104) and MBPS groups relative to PBS. SN samples displayed the greatest transcriptional response specific to MBP(84-104) in both sexes. Transcription patterns in female and male nerves exhibited a significant overlap. In contrast, fewer DE genes were identified in DRG and DSC, whereas the majority exhibited sexually dimorphic expression. In female DRG and DSC, we recorded a higher number of up-regulated relative to down-regulated genes, whereas males demonstrated a higher number of down-regulated relative to up-regulated genes in response to MBP(84-104).

The principal component analysis of the top DE genes (Fig. 2*c*) indicates that in sciatic nerve, MBP(84-104) was responsible for 96.2% of the variance of the top DE genes; only 3.5% variance was due to sex. Conversely, in DRG, sex was responsible for 41.4% variance, whereas MBP(84-104) contributed to 30% variance of the top DE genes. In the spinal cord, neither sex nor MBP(84-104) treatment contributed significantly to the variance of the top DE genes.

The hierarchic clustering analysis of the top DE genes in SN, DRG, and DSC (Fig. 2*d*) exhibited notable sexual dimorphism in response to the injection (IS PBS group) in all tissues. It further confirmed that the vast transcriptome changes in female and male SN in response to MBP(84-104) were absent in the PBS group. Over 1,180 top up-regulated DE genes in SN, regardless of sex, were co-expressed in the corresponding DRG. Gene list enrichment analysis using ToppGene Suite (43) predicted that the SN/DRG co-expressed genes related to anterograde transsynaptic and ion channel signaling (data not shown). To further explicate the site-specific changes caused by IS MBP(84-104), we conducted predictive analysis of the biological functions and canonical signaling pathways in SN, DRG, and DSC using the curated content of the ingenuity pathway analysis (IPA) knowledge base (Qiagen Bioinformatics, Redwood City, CA, USA).

Robust signaling changes with minor sexual dimorphism in nerve exposed to MBP(84-104)

At day 7 post-injection, IS MBP(84-104), but not MBPS, stimulated robust signaling activity in male and female SN (Figs. 3 and 4). Sexually dimorphic regulation of biological processes was detected by gene enrichment analysis (Fig. 3*a*) that revealed induction of transcriptional activity related to cell projection morphogenesis and vesicular localization preferentially active in female SN, whereas neurotransmitter secretion and transport were more dominant in male SN (Fig. 3*a*). The canonical pathways in SN, induced selectively by IS MBP(84-104), but not MBPS (fold-change relative to PBS, Fig. 3*b*) displayed mild sexual dimorphism related to nociceptive, immune, bioenergetics, and lipid metabolism signaling, detailed below.

Nociceptive pathways—These pathways stimulated by MBP (84-104) in both sexes displayed slightly higher activation Z-scores in female as compared with male SN (Fig. 3*b*). These pathways were categorized as *neuropathic pain signaling*, *glutamate receptor signaling*, *calcium signaling*, and *synaptic long-term potentiation* pathways. A detailed observation of the pathways in female SN showed induction in voltage-gated Ca^{2+} channel (VGCC) family, glutamate ionotropic receptor (GLUR5), *N*-methyl-D-aspartate receptor, and serotonin receptor (5HT3R) transcripts (Fig. 4, *a* and *b*). Notably, MBP (84-104) induced calmodulin-dependent kinase (CAMK)II/calcineurin signaling, potentially based on the established MBP-calmodulin interaction (21, 22). SN of both sexes induced *opioid signaling* and *endocannabinoid inhibition* pathways (Fig. 3*b*) associated with the opioid SIGMAR1 and endocannabinoid CNR1 receptor expression.

Immune pathways—Immune pathways, including T cell-related interleukin (IL)-22 signaling and 4-1BB signaling in T lymphocytes, were activated in response to MBP(84-104) in both sexes, with higher activation scores in female SN (Fig. 3*b*). Innate immune pathways, related to inflammasome, neuroinflammation, Toll-like receptor, and pro-nociceptive cytokine signaling were not significantly regulated at day 7 after IS MBP (84-104) relative to MBPS in female or male SN (Fig. 3*b*). These data confirm our finding of T cell homing in SN after IS MBP (84-104) but not MBPS (29, 32).

Lipid and energy metabolism pathways—Lipid and energy pathways, including *oxidative phosphorylation*, *Krebs (TCA) cycle*, *gluconeogenesis* and *glycolysis* pathways, were selectively induced by IS MBP(84-104) in SN of both sexes, with higher Z-scores in male SN (Fig. 3*b*). Critical components of the mitochondrial respiratory chain, including cytochrome *c* oxidases (COX8B, COX4I2, and COX17 subunits), ATP synthase (ATP5MG), NADH dehydrogenases (NDUFA8, NDUFB2, NDUFS7, and NDUFB7 subunits), and ubiquinol-cytochrome *c* reductase (UQCRQ and UQCR10 subunits) were prevalent in male SN (Fig. 4*c*). The higher metabolic ergogenic activity in SN was associated with absence of pain behavior in males and associated with positive regulation of *peroxisome proliferator-activated receptor (PPAR)/retinoid X receptor (RXR) signaling* known to balance antioxidant redox, immune, and fatty acid oxidation states (44) (Fig. 3*b*). Mildly elevated *liver X receptor (LXR)/RXR* pathway in male *versus* female SN (Fig. 3*b*) suggests a more efficient cholesterol efflux in males. In female SN, IS MBP(84-104) activated the *superpathway of cholesterol biosynthesis* signaling (Fig. 3*b*) associated with induction in 3-keto-steroid reductase (HSD17B7) and 7-dehydrocholesterol reductase (DHCR7) (Fig. 4*d*). These data agree with our recent finding that MBP(84-104) regulates mitochondrial cell metabolism (34) and further suggests this process is sexually dimorphic.

Vesicle localization—The vesicle localization process was selectively active in female SN exposed to MBP(84-104) (Fig. 3*a*) and reflected induction of nearly 30 genes, including kinesin family members (KIF13A, KIFC1, KIF5B, and KIF1A),

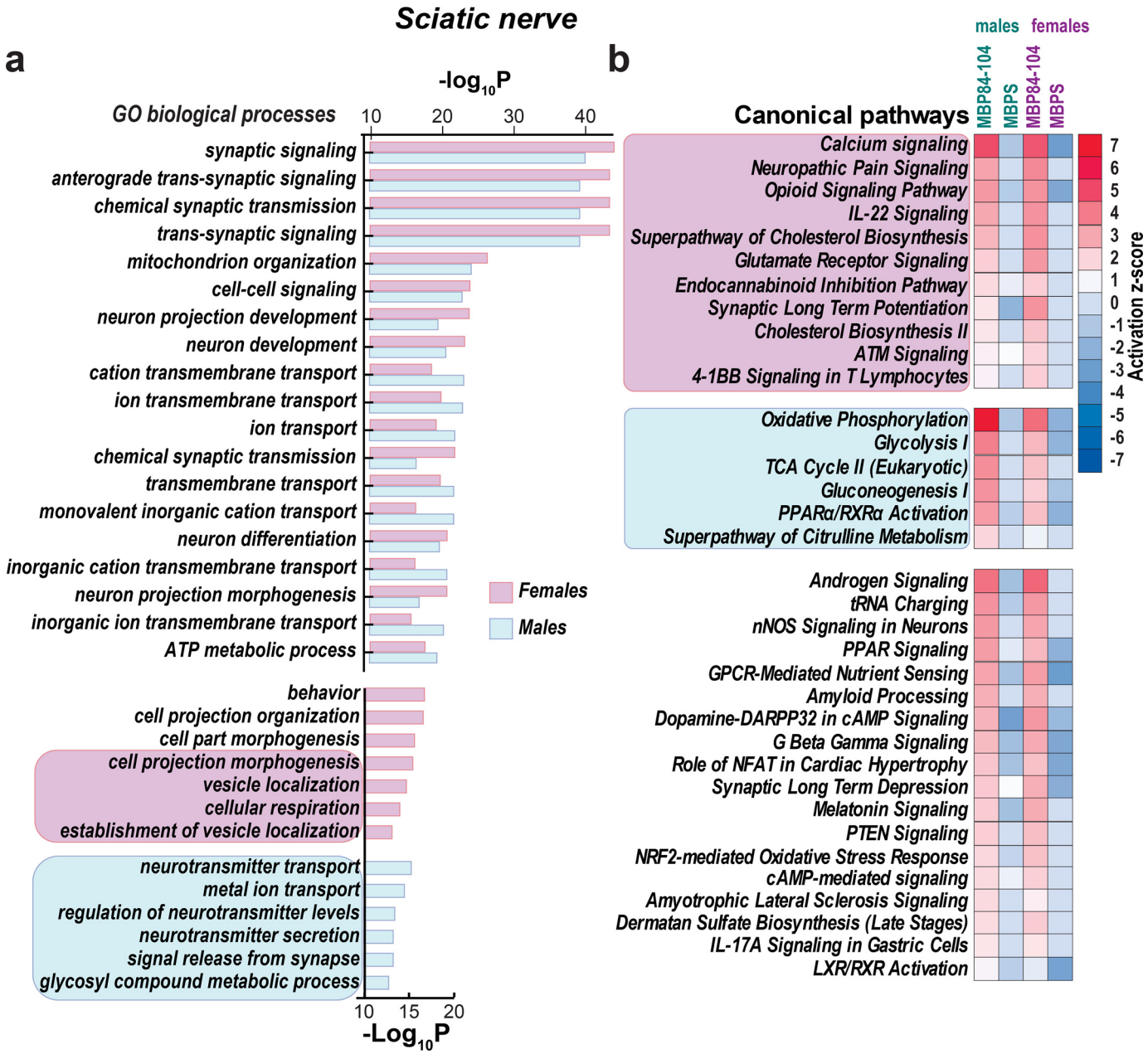

Figure 3. GO biological processes and ingenuity canonical pathways in female and male nerve after IS MBP(84-104). *a,* Gene ontology (GO) biological processes were determined by functional enrichment meta-analysis (ToppGene Suite) using lists of up-regulated DE genes in female and male SN after IS MBP (84-104) or IS MBPS relative to PBS. Enrichment significance cutoff is $p \leq 0.05$ (after Bonferroni correction). *Bars* represent -$\log_{10}$P of the most significant biological processes in females (*purple*) and males (*light blue*). *b,* canonical pathways (Ingenuity IPA). The regulation Z-scores represent activated (*red*) or deactivated (*blue*) pathways according to the color scale. Selected sexually dimorphic pathways are highlighted.

exocyst complex component EXOC4, involved in targeting exosomes to docking sites on plasma membrane, protein kinase C (PRKCA), MAPK15, nicotinic cholinergic receptor CHRNA3 (45), dopamine receptor DRD1, and neurotransmitter release-related ERC1 and ERC2 (46). Hence, MBP(84-104) selectively activates vesicular transport in female nerve.

Major sexual dimorphism in DRG and spinal cord after IS MBP (84-104)

Next, we analyzed the changes in ipsilateral DRG (Fig. 5) and DSC (Fig. 6) samples at day 7 post-injection produced by IS MBP(84-104) but not MBPS (fold-change relative to PBS). In both ipsilateral DRG (Fig. 5) and DSC (Fig. 6), IS MBP(84-104) regulated a fewer number of DE genes compared with the nerve, but the majority of the DE genes exhibited sexually dimorphic expression. A striking observation is that transcriptional activity underlying biological processes in DRG (Fig. 5*a*) and DSC (Fig. 6*a*) are observed only in females post-IS MBP(84-104). Male DRG and DSC post-IS MBP(84-104) exhibited no transcriptional activity associated with known biological processes. Our further gene list enrichment analysis using ToppGene Suite identified the following sex-specific canonical inflammatory and

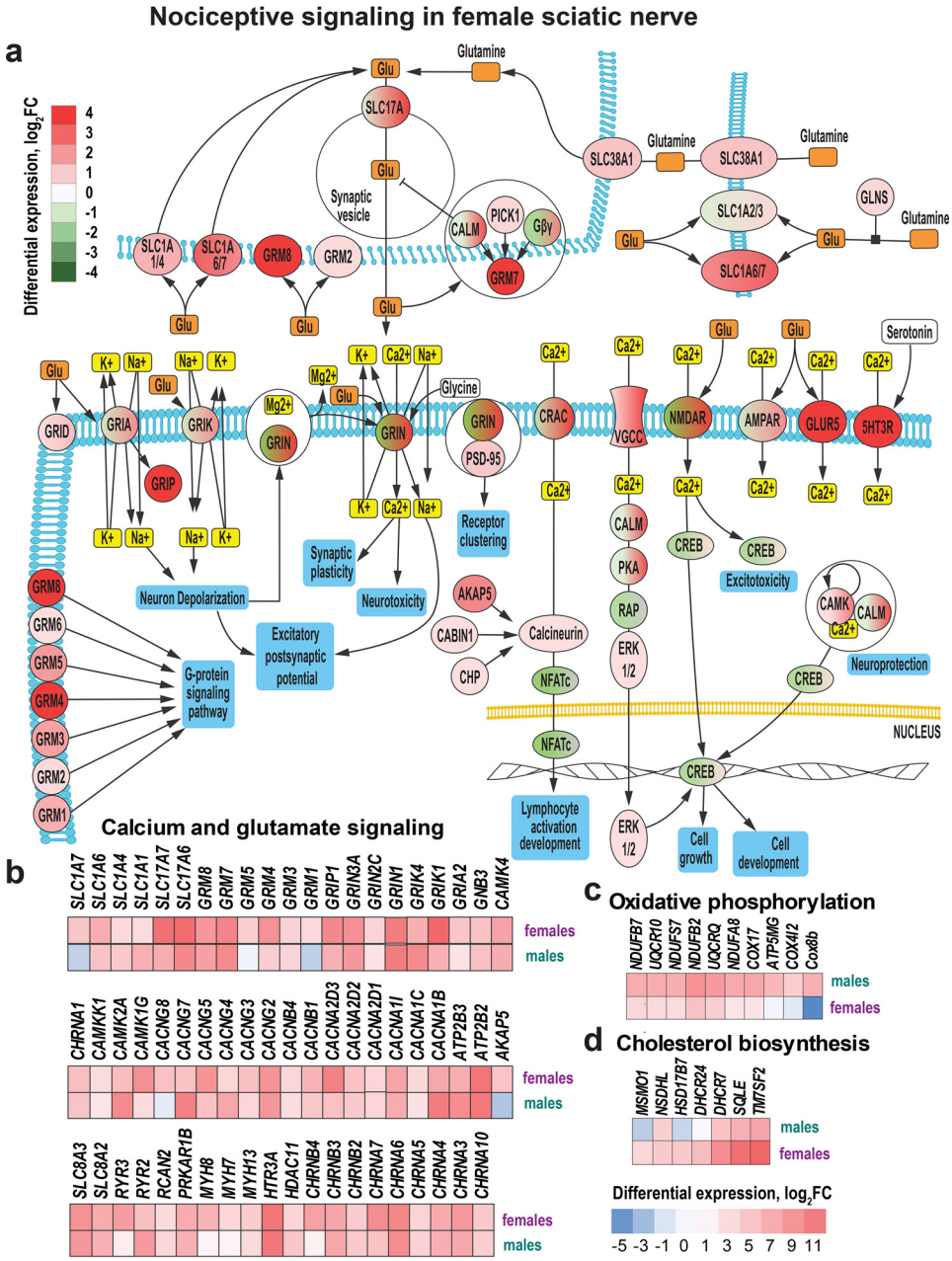

Figure 4. Nociceptive signaling in female nerves after IS MBP(84-104). *a,* schematic presentation of a SN-immune synapse after IS MBP(84-104). Pathway components (molecules and complexes) are displayed as *circles*; *arrows* indicate molecular interactions according to Ingenuity IPA (Qiagen). *Red* and *green* colors correspond to up- and down-regulated DE genes, respectively, relative to PBS and according to the scale. Gradient colors indicate regulation of individual components of protein complexes. Downstream biological processes are highlighted in *blue*. Heat maps of *(b)* calcium and glutamate signaling genes, (*c*) oxidative phosphorylation genes, and (*d*) cholesterol biosynthesis genes after IS MBP(84-104) relative to IS PBS in female and male SN. Color scale corresponds to log_2FC.

nociceptive signaling pathways in DRG and DSC regulated by IS MBP(84-104).

Immune system pathways—The immune system pathways were induced in female DRG (Fig. 5) and DSC (Fig. 6) after IS MBP(84-104). In female DRG, leukocyte differentiation and activity GO processes (Fig. 5*a*) correspond to *leukocyte extravasation signaling* (Fig. 5*b*) related to leukocyte rolling and transmigration related genes (Fig. 5*c*). Female DRG displayed pro-inflammatory *p38/MAPK*, *iNOS,* and *TNFR1 signaling* activity. Selectively in female DSC, IS MBP(84-104) induced *CD28 signaling in T helper cells*, *protein kinase C* (*PKC*) *signaling* in *lymphocytes*, *B cell receptor signaling*, *IL-8, iNOS, neutrophil,* and *MAPK signaling* (Fig. 6*b*). In male DRG (Fig. 5*b*) and DSC (Fig. 6*b*), immune pathways were inactive in all groups, with the exception of *macrophage* migration inhibitory factor (MIF) regulation of innate immunity and nuclear factor of activated T cells (NFAT) in the immune response induced in DSC after IS MBP(84-104) (Fig. 6*b*). In male DRG (Fig. 5*b*) and DSC (Fig. 6*b*), IS MBP (84-104)-induced phosphoinositide 3-kinase (PI3K)/AKT signaling, suggesting an active regulatory process may exist in males that is absent in females.

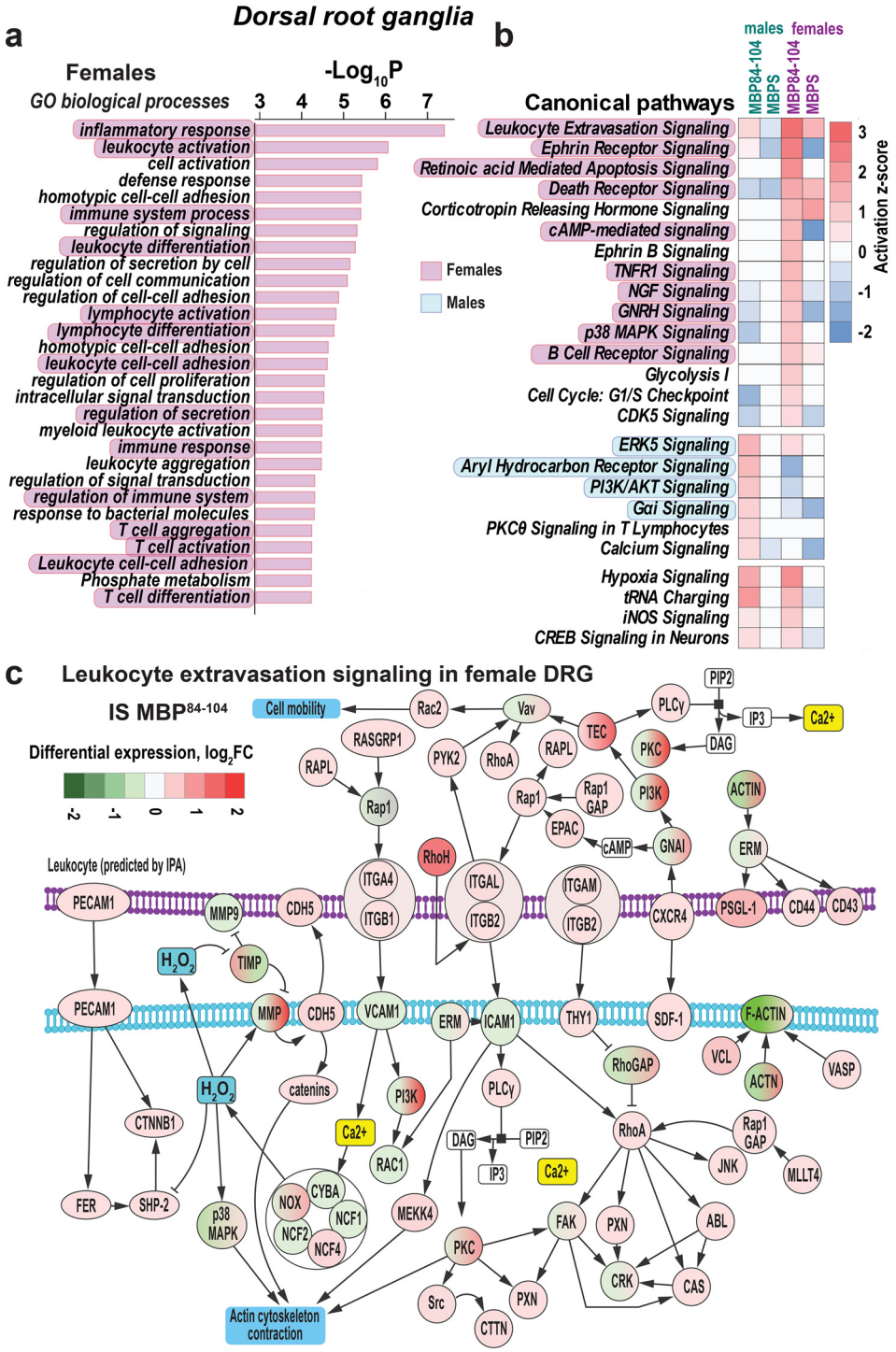

Figure 5. GO biological processes and canonical pathways in DRG after IS MBP(84-104) are female-dominant. *a,* GO biological processes determined by functional enrichment meta-analysis (ToppGene Suite) positively regulated in female DRG (FC $\geq$ 2) after IS MBP(84-104) or MBPS relative to PBS. Male DRG displays no significant activation of biological processes. Enrichment significance cutoff is $p \leq 0.05$ (after Bonferroni correction). *Red bars* represent -$\log_{10}$P of the most significant biological processes in female DRG. Female-specific biological processes are highlighted. *b,* regulation of canonical pathways in female and male DRG (Ingenuity IPA). Heat map of the activation Z-scores, colors correspond to positive (*red*) or negative (*blue*) regulation of canonical pathways according to the scale. Sexually dimorphic canonical pathways in females (*purple*) and males (*light blue*) are highlighted. *c,* schematic presentation of leukocyte extravasation signaling induced by IS MBP(84-104) in female DRG. Pathway components (molecules and complexes) are displayed as *circles*; *arrows* indicate molecular interactions according to Ingenuity IPA (Qiagen). Downstream biological processes are highlighted in *blue*. *Red* and *green* colors correspond, respectively, to up- and down-regulated DE genes relative to IS PBS according to the color scale ($\log_2$FC). Gradient colors indicate regulation of individual components of protein complexes.

Estrogen receptor (ESR) 1-nociceptive signaling—Gene enrichment analysis demonstrates remarkable sexual dimorphism in transcriptional activity of nociceptive pathways in ipsilateral DSC at day 7 after IS MBP(84-104), but not MBPS (fold-change relative to PBS) (Fig. 6). In spinal cord, IS MBP(84-104) regulated a vast signaling network convergent on Ca^{2+} homeostasis

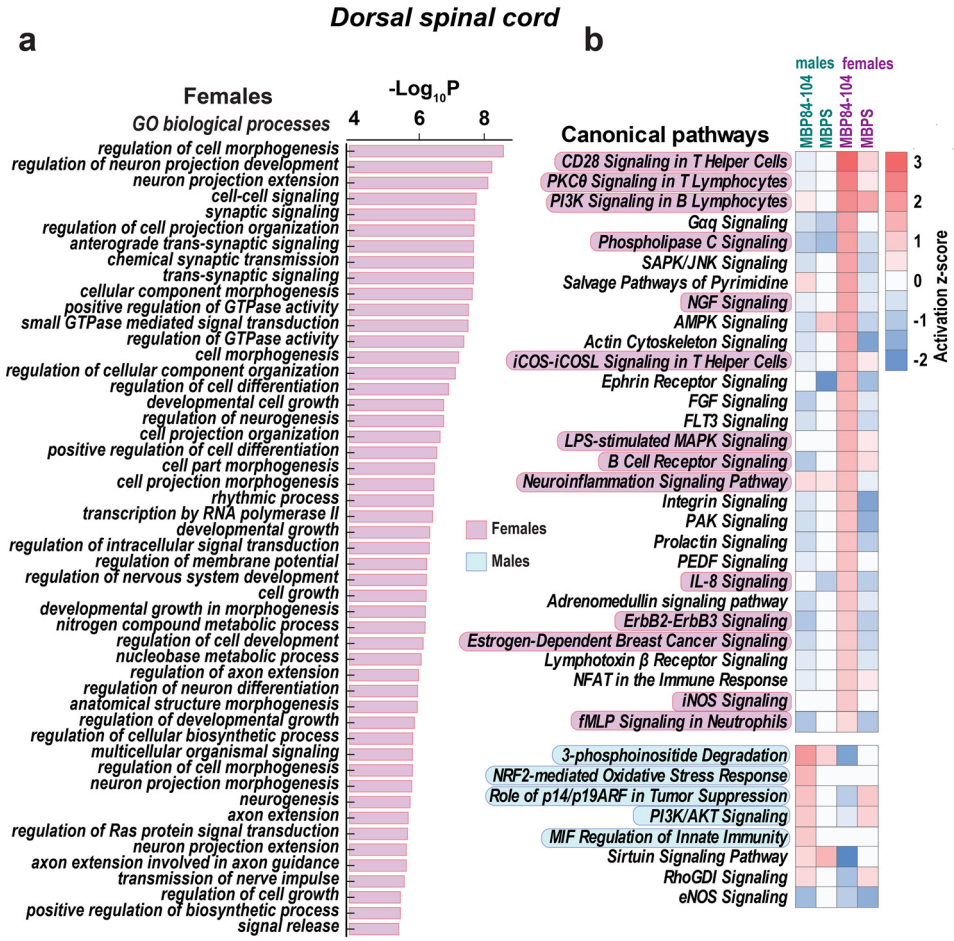

Figure 6. GO biological processes and canonical pathways in spinal cord after IS MBP(84-104) are female-dominant. *a,* GO biological processes determined by functional enrichment meta-analysis (ToppGene Suite) positively regulated in female dorsal spinal cord (DS(C) FC $\geq$ 2) after IS MBP(84-104) or MBPS relative to PBS. Enrichment significance cutoff is $p \leq 0.05$ after Bonferroni correction. *Red bars* represent -$\log_{10}$P of the most significant biological processes in females. *b,* canonical pathways in female and male DSC (Ingenuity IPA). Heat maps illustrate the activation Z-scores, colors correspond to positive (*red*) or negative (*blue*) regulation of canonical pathways according to the scale. Selected canonical pathways in females (*purple*) and males (*light blue*) are highlighted.

in a sex-dependent manner. This network includes VGCC, CAMKII/calcineurin, and glutamate AMPA/mGLU receptor signaling, co-regulated (induced in females and suppressed in males) by estrogen receptor ESR1 and PLC-activated endoplasmic reticulum inositol trisphosphate receptor (IP3R) signaling cascades.

These findings support the multicellular "shared amplifier" paradigm of the ESR1/IP3R system contribution to female-prevalent hyperalgesic priming via IP3-mediated Ca^{2+} release from endoplasmic reticulum (ER) and Ca^{2+} signal amplification in spinal cord (47, 48). According to this paradigm, mechanical allodynia in females is therapeutically sensitive to intrathecal (IT) administration of xestospongin C, a specific and reversible IP3R inhibitor that inhibits IP3-mediated Ca^{2+} release from ER stores (47, 48). To test this model, we used von Frey testing to confirm mechano-allodynia at day 10 after IS MBP(84-104) in female mice. Administration of IT xestospongin C (1 nmol), but not 10% DMSO vehicle, mitigated IS MBP(84-104) allodynia for ~2 h (Fig. 7*b*). Intraperitoneal (i.p.) gabapentin (100 mg/kg), used as control anti-allodynia therapy effective in a clinical setting (49) and IS MBP(84-104) in female rats (32), effectively attenuated IS MBP(84-104) allodynia in female mice (Fig. 7*b*). Thus, the nerve exposure of autoantigenic myelin peptides initiates ESR1-nociceptive signaling in females (presumably due to high estrogen levels) that can be targeted by the endoplasmic reticulum IP3R inactivation in cells of spinal cord.

Discussion

Despite the high regenerative capacity of damaged peripheral nerve, an intractable neuropathic pain, mechano-allodynia, may persist for years after nerve repair. In evidence for autoimmune pathogenesis of mechano-allodynia pain specifically in females, we here demonstrate that nerve exposure to a pure autoantigenic MBP peptide, endogenously released post-injury (26, 28–31, 50), initiates female-specific mechano-allodynia. Our unbiased, comparative genome-wide transcriptional view of the respective sciatic nerve, DRG, and spinal cord of both sexes reveals striking multisite, sexually specific molecular changes after nerve MBP(84-104) exposure, leading to mechano-allodynia in females and no change in mechanical sensitivity in males. This dimorphism represents several organizing principles revealing a 3-tier signaling program, discussed below and illustrated in Fig. 8.

Tier 1: sex-specific utilization in lipid and cell energy metabolism

Myelin is a lipid-rich multilamellar membrane formed by Schwann cells and maintained via interactions of cationic MBP with anionic membrane phospholipids, such as PIP2 (23), and anionic proteins, including actin, tubulin, and Ca^{2+}-calmodulin (21, 22). In agreement, we find the MBP(84-104)-induced mechano-allodynia is diminished with charge reduction by substitution of basic histidine 89 for amphoteric glycine 89 (30). Strong transcriptional response in nerves of both sexes suggests

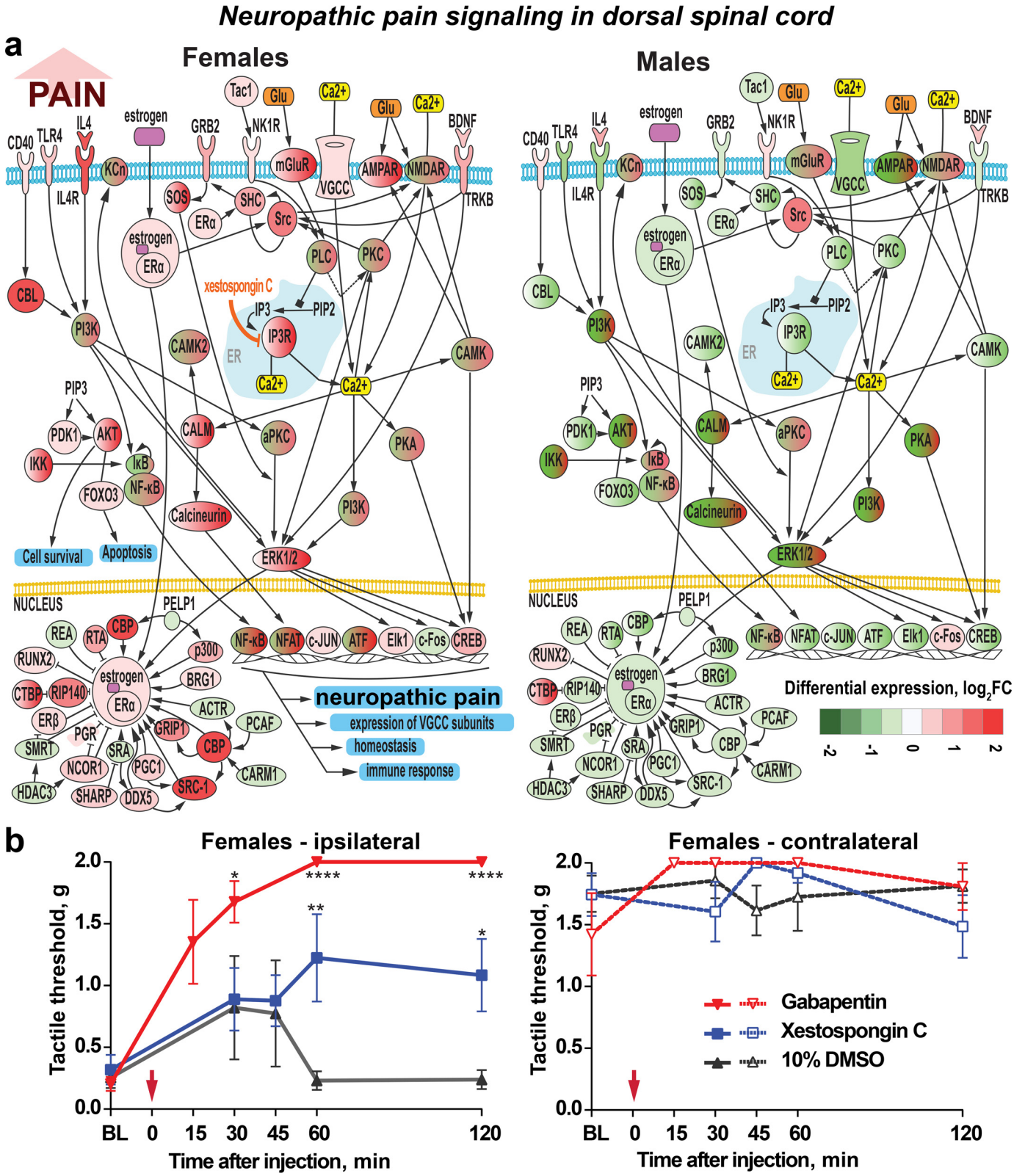

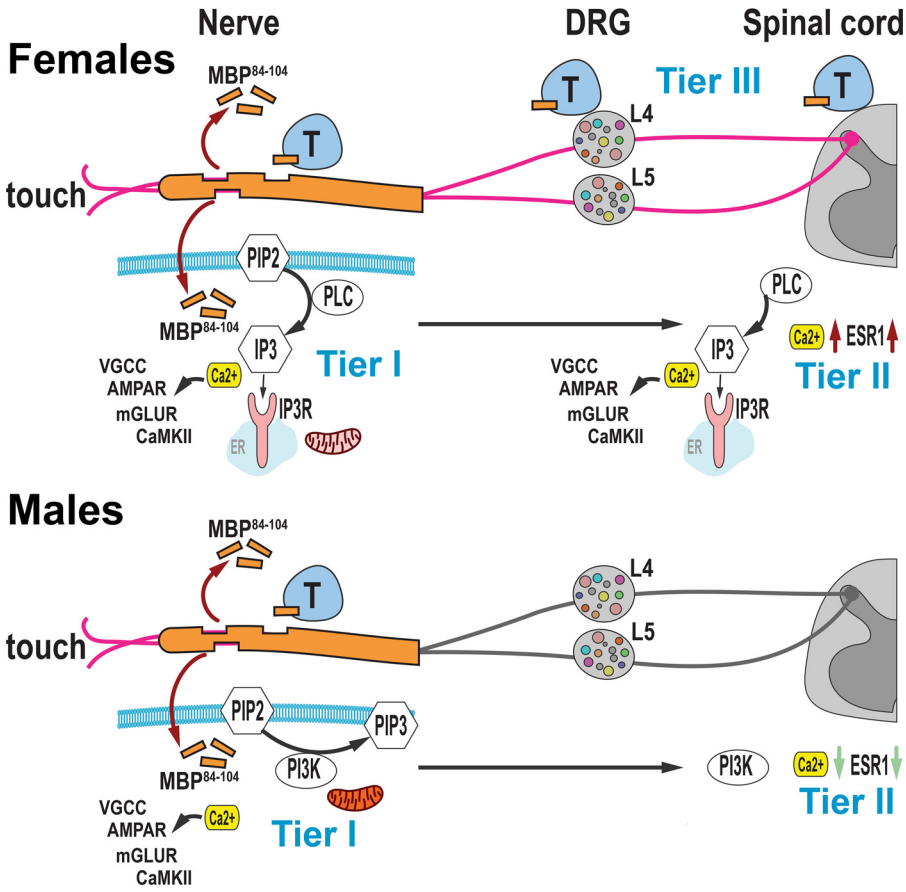

Figure 8. An autoantigenic myelin peptide drives a 3-tier program to sexually dimorphic (female-specific) neuropathic pain. Myelin ensures propagation of tactile sense via mechano-sensory neurons from peripheral nerve to DRG then spinal cord. After nerve injury, proteolytic myelin fragmentation exposes a functionally distinct autoantigenic MBP(84-104) peptide in both sexes. MBP(84-104) triggers an integrative, sex-specific, 3-tier signaling program leading to mechanical hypersensitivity selectively in females: *tier I,* phospholipid metabolism: based on its interaction with PIP2 phospholipid (50), MBP(84-104) induces PLC-driven PIP2 hydrolysis to IP3 in females and PI3K-driven PIP2 to PIP3 synthesis in males. *Tier II*, ESR1/nociceptive co-regulation: in female spinal cord, sustained ESR1/IP3 receptor (IP3R) co-activation (*red arrows*, due presumably to high estrogen levels relative to male) results in IP3R-mediated Ca^{2+} release from ER yielding Ca^{2+}-dependent nociceptive signaling via VGCC, AMPAR, mGLUR, and CaMKII increase. This ESR1/IPR3/nociception loop is repressed in male spinal cord (*green arrows*). *Tier III,* autoantigenicity: the autoantigenic MBP(84-104) epitope exposure causes T cell (*T*) activation in nerves of both sexes. T cell-related activity advances to DRG and spinal cord in females, whereas stays localized to nerves in males. The three-tier signaling program can be interrupted by spinal IP3R inactivation (Fig. 7*b*) and (48) and T cell deletion (29).

efficient MBP(84-104) uptake regardless of sex. Potential sex differences in cell membrane lipid composition or function may underlie sexual dimorphism of nociception induced by MBP. The cell type specificity of signaling activity obscured by bulk RNA-seq remains to be elucidated. In the injected nerve, Schwann cells constitute over 80% of cell population, whereas immune cells (particularly, macrophages and lymphocytes), fibroblasts, and endothelial cells may contribute to the present findings (51, 52).

According to the established MBP-PIP2 interactions (23), MBP(84-104) causes an increase in PLC (which hydrolyzes PIP2 to IP3) in females and increase in PI3K (which mediates PIP2 to PIP3 synthesis) in males (tier 1). These changes may underlie subsequent changes, discussed in tier 2, below and illustrated in Fig. 8.

MBP(84-104) seems to induce a high level of ergogenic metabolic activity in male compared with female nerves, including Krebs/TCA cycle, glycolysis and oxidative phosphorylation signaling relative to females. In contrast, female nerves show increased superpathway of cholesterol biosynthesis signaling and reduced cholesterol efflux *LXR/RXR* signaling. Generally,

Figure 7. IS MBP(84-104) causes striking sexual dimorphism in spinal nociceptive signaling. *a,* neuropathic pain network of PLC/IP3R/VGCC axis and ESR1/p300/CBP axis after IS MBP(84-104) in females (*left panel*) and males (*right panel*). Pathway components (molecules and complexes) are displayed as *circles*, *arrows* indicate molecular interactions according to Ingenuity IPA (Qiagen). Downstream biological processes are highlighted in *blue*. *Red* and *green* colors correspond to up- and down-regulated DE genes according to the color scale (log_2FC). Gradient colors indicate regulation of individual components of protein complexes. Threshold FC ≥ 2, $p \leq 0.05$. IP3R is a site of xestospongin C action in females (*orange line*). *b*, von Frey testing in female mice ipsilateral (*left panel*) and contralateral (*right panel*) to IS MBP(84-104) (30 μg in 3 μl). At day 10 after IS MBP(84-104), IT administered IP3R inhibitor, xestospongin C (X2628, 1 nmol/5 μl, $n = 5$), but not vehicle 10% DMSO (5 μl, $n = 4$), attenuated the established allodynia. Control i.p. gabapentin (100 mg/kg, $n = 3$) also attenuated IS MBP(84-104) allodynia. The mean withdrawal tactile thresholds are in gram force (g) $\pm$ S.E.; two-way ANOVA (*b, left*: treatment $\times$ time $f = 3.220$, $p = 0.0162$, time $f = 9.681$, $p = 0.0002$, treatment $f = 15.94$, $p = 0.0011$, subject $f = 1.125$, $p = 0.3797$; *b, right*: treatment $\times$ time $f = 1.407$, $p = 0.2482$, time $f = 1.346$, $p = 0.2803$, treatment $f = 0.2114$, $p = 0.8134$, subject $f = 3.109$, $p = 0.0107$) with Dunnett's post hoc test: *, $p \leq 0.05$; **, $p \leq 0.01$; ****, $p \leq 0.0001$ relative to the DMSO control. Not all groups were tested at the 15- and 45-min time points; these time points are shown in the graph, but were not included in the data analysis. *Red arrows* indicate drug administration.

peripheral nerves resemble other tissues that in response to stress, utilize carbohydrate and protein as an energy source in male cells, and lipid in females (53). In DRG and Schwann cell cultures, we find that MBP(84-104) controls cell energy metabolism and the lactate/glucose ratio via potential interaction with lactate dehydrogenase and mitochondrial voltage-dependent anion-selective channel protein (VDAC)-1 (34), and by modulating the ATPase activity of cyclin-dependent kinases (30).

Tier 2: sex-specific co-regulation of estrogen receptor, ER stress, and nociceptive signaling

Presumably due to inherently high estrogen level in females relative to males, the female-specific PLC activity in tier 1, the estrogen receptor ESR1 co-activation with IP3R causes IP3R-mediated release of calcium ions from ER stores, leading to imbalance in Ca^{2+} homeostasis after nerve MBP(84-104) exposure. This further potentiates the vast Ca^{2+}-dependent nociceptive signaling via VGCC, AMPAR, mGLUR, and CAMKII/calcineurin up-regulation exclusively in the female spinal cord, as illustrated in Fig. 8. The cells responsible for the induction of the predicted pathways remain to be elucidated. The female-specific hyperalgesic priming has been previously attributed to co-regulation of ESR1/IP3R activity via imbalance in Ca^{2+} homeostasis (48).

Conversely, the ESR1/IP3R-nociceptive genes are suppressed in the male spinal cord presumably due to inherently low estrogen levels in males relative to females. Interestingly, many such nociceptive genes are locally up-regulated in male and female nerves exposed to MBP(84-104). This effect is not seen after PBS or MBPS injection, suggesting that in males, MBP(84-104) may stimulate an active analgesia (or an adverse hypoalgesia) mechanism. The present data set provides rich information on the transcriptional landscapes in MBP(84-104)-induced nerve changes, which could be useful for further data mining of the analgesia mechanism in males to develop new anti-allodynia approaches in both sexes. In contrast to the PLC-driven PIP2 hydrolysis to IP3 and activation of the IP3R/ESR1-nociceptive signaling, males induce PI3K activity (expected to mediate PIP2 to PIP3 synthesis) in the nerve, DRG, and spinal cord (Fig. 8). The cell specificity of the predicted signaling activity remains to be determined. Xestospongin C, whereas deemed a selective IP3R inhibitor, has the ability to inhibit the Ca^{2+}-ATPase of the ER causing depletion of both IP3- and ryanodine-sensitive Ca^{2+} stores (54, 55). Furthermore, mobilization of Ca^{2+} stores in glia (microglia, astrocytes) and neurons may result in distinct pro- and anti-nociceptive activities.

Male nerves exhibited no exosomal and vesicular localization gene activity seen in female nerves. This may suggest that MBP (84-104) exposure induces a pro-nociceptive retrograde axonal vesicular transport from the nerve to DRG in females that is absent in males. The transcriptomic analysis does not reflect activity of pro- and anti-nociceptive proteins, lipids, and metabolites. Future studies must elucidate the cellular, subcellular, and molecular mechanism that link estrogen receptor, ER stress, and nociceptive changes leading to sexual dimorphism in mechanical hypersensitivity.

Tier 3: autoimmune mediation of neuropathic pain is prevalent in females

Neuropathic pain depends on activity of immune cells (*e.g.* macrophages, lymphocytes) and immunocompetent glia (Schwann cells, satellite glia, microglia, and astrocytes) (52). We find T cell-related signaling activity in both male and female nerves (albeit IL-22 and 4-1BB signaling pathways were female-prevalent). The female-specific MBP(84-104) allodynia is accompanied by sustained T cell-related signaling extending to DRG and spinal cord exclusively in females (Fig. 8), potentially contributing to female-specific T cell mediation of mechano-allodynia in mice with peripheral nerve injury (11, 19), known to release the autoantigenic MBP(84-104) (26, 28–31, 50).

IS MBP(84-104) does not model mechano-allodynia in male mice. In male mice with nerve injury, mechano-allodynia is thought to depend on activity of spinal microglia (11). To some degree, mechanical-allodynia in males may respond to T cell targeting (15–18), including by immunization with an altered/mutant MBP ligand (56), depending on species, strains, and types of neuraxial injury. In males, T cell-related signaling was apparent in nerve, at the site of nerve exposure, but not in DRG or spinal cord. These data suggest a more complex T cell function in neuropathic pain. Indeed, prior data using both sexes has implicated T helper (Th)1 and Th17 cells infiltrating the injured peripheral nerve and the segmental spinal cord in the development of mechano-allodynia (15–18). The studies elucidating sex differences in T cell regulation after IS MBP(84-104) are ongoing.

The bulk RNA-seq that generated data from mixed cell types and the changes were not reliably attributed to different cell types. It is plausible that T cells access DRG lacking a neurovascular barrier (57). Non-immune cells may contribute to adaptive immune pathway activity, particularly in spinal cord with intact blood-spinal cord barrier. In female rats exposed to IS MBP(84-104), we find that astrocytes and deep dorsal horn neurons of ipsilateral spinal cord contribute to immune/IL-6–related production (32). Using female athymic nude rats lacking mature T cells, we have conclusively established that maintenance of IS MBP(84-104) allodynia is T cell-dependent (29). It is presumed that via MBP(84-104) antigen-presenting nerve Schwann cells and macrophages assist in T cell homing to mechanosensory neurons leading to cytokine-mediated sensitization (29). The site and mechanisms of T cell function remain to be determined.

Autoimmune disorders, including MBP-mediated multiple sclerosis (58), are far more prevalent in women (59, 60). We believe MBP(84-104) is the first autoantigenic epitope sequence shown to induce mechano-allodynia selectively in female, but not male, mice. These data support autoimmune pathogenesis of this refractory pain phenotype specifically in females and the role of MBP(84-104), endogenously released in peripheral nerve after a focal trauma (26, 28–31, 50), as a prototype T cell epitope in mechano-allodynia. The N-terminal 2-18 MBP epitope produced no allodynia after IS delivery (29), emphasizing the importance of the invariant α-helix ^{87}VVHFF^{91} MBP motif.

IS MBP(84-104) recapitulates focal nerve injury

IS MBP(84-104) partially models events induced by endoneurial release of central MBP peptides during focal nerve injury (26, 28–31, 50). In contrast to nerve injury, IS MBP(84-104) allodynia is not accompanied by the acute degenerative or reparative processes (29, 32), making it a more specific model of this intractable pain state. It is logical to assume that nerve injury induces a plethora of additional signaling cascades not recapitulated by IS MBP(84-104) that affect both males and females and mediates allodynia in males.

IS MBP(84-104) causes mechanical, but not heat, hypersensitivity (29, 32) consistent with myelin-targeted mechanisms of sensitization of mechano-sensitive (inherently, myelinated) A-afferents over heat-sensitive/nociceptive (inherently, unmyelinated) C-fibers. That an equal dose of MBP(84-104) causes female-specific allodynia confirms that downstream mechanisms and not the amount of MBP(84-104) produced in nerve determines sexual dimorphism of pain behavior. IS MBP (84-104) did not induce innate immune pathways, as seen here and previously (29, 30, 32). Endogenous release of MBP peptides in nerve post-injury is mediated by matrix metalloproteinases (29, 50).

The pathogenic action of the MBP peptides is distinct from that of the full-length MBP in healthy tissues. After peripheral nerve injury, the MBP peptides translocate from the myelin internode toward the node (26, 28–31) and escape macrophage phagocytosis (28), potentially by evading the scavenger low-density lipoprotein receptor-related protein 1 (LRP-1), which binds the full-length MBP (34). Nerve injury, required to release the cryptic epitopes concealed within the intact myelin from immunosurveillance (29), likely produces unique MBP peptide interactors, not captured by our IS MBP(84-104) model. Given the robust IS MBP(84-104) allodynia (produced by IS injection in intact nerve), we argue the injury-specific interactors are not essential to allodynia. The pro-algesic action of the MBP peptides may employ the full-length MBP interactors, including phospholipids.

From a clinical perspective, in addition to focal nerve trauma, MBP(84-104) is released in painful neurodegenerative and autoimmune demyelinating states, including multiple sclerosis (30, 31). In support of autoimmune pathogenesis of mechano-allodynia, we find anti-MBP(84-104) autoantibodies in the serum of female rats with focal nerve injury and women with multiple sclerosis (31). The pathogenic role of these autoantibodies in pain is under current investigation. Other demyelinating triggers, including drugs, toxins, or pathogens, may produce MBP-mediated pain states. In addition, MBP epitope release via targeted proteolysis is seen before demyelination and after remyelination (29–31), potentially implicating MBP in highly prevalent idiopathic pain states. Based on its high structural homology with muscarinic M2 acetylcholine receptor, MBP(84-104) may contribute to complex regional pain syndrome (33).

In conclusion, the present study implicates for the first time a myelin autoantigen in sexually dimorphic regulation of neuropathic pain. The female-specific T cell mediation of mechano-allodynia (11) may represent at least in part an autoimmune myelin-targeted sensitization of myelinated mechanosensitive afferents caused by integrative dysregulation of lipid/cholesterol metabolism and calcium-dependent nociception via increased estrogen receptor activity. Our rigorous molecular, cellular, and functional validation of the predicted pathways is ongoing. Our robust data, new concepts, and the unique comprehensive open-access database aim to improve diagnostic and therapeutic strategies of neuropathic pain management based on sex.

Experimental procedures

Reagents

General reagents were purchased from Thermo Fisher Scientific (Carlsbad, CA, USA). MBP(84-104) (ENPVVHFFKNIVTPRTPPPSQ) and scramble (MBPS, NKPQTNVVEPFHRTFPIPPVS) peptides, derived from the human MBP sequence (GenBank™ AAH08749), protected by N-terminal acetylation and C-terminal amidation, were synthesized and purified using HPLC by GenScript (Piscataway, NJ, USA). Gabapentin was from Toronto Research Chemicals (Ontario, Canada), and xestospongin C (X2628) was from Sigma-Aldrich.

Animal model

C57BL/6 mice (8–10-week-old adult, Envigo Laboratory, Huntingdon, United Kingdom) were housed in a temperature-controlled room (~22 °C) on a 12-h light/dark cycle with free access to food and water. All procedures and testing were conducted during the light cycle. Under isoflurane anesthesia (Isothesia, Henry Schein, Melville, NY, USA), the common sciatic nerve was exposed unilaterally at the mid-thigh level through a gluteal muscle-splitting incision. A single endoneurial bolus injection of the MBP(84-104) and MBPS peptides (30 μg in 3 μl of PBS, each) was performed into the sciatic nerve fascicle (IS) using a 33-gauge needle on a Hamilton syringe. Sciatic nerve (5-mm injection site fragment), lumbar (L)4-5 DRG (pooled), and L1-L6 spinal cord, dorsal quarter (DSC), and ipsilateral to injection were excised and stored in RNA-later (Thermo Fisher Scientific) at −20 °C. Animals were sacrificed using Beuthanasia IP (Merck Schering-Plough Animal Health, Kenilworth, NJ, USA). All animal procedures were performed according to the PHS Policy on Humane Care and Use of Laboratory Animals, ethical guidelines of the International Association for the Study of Pain and the protocol approved by the Institutional Animal Care and Use Committee at the University of California, San Diego.

von Frey testing

Behavioral testing was performed by the experimenter blinded to treatment groups. The animals were randomized and stratified to treatment groups and habituated to the testing environment prior to baseline tests. For assessment of mechanical withdrawal threshold, mice were placed in individual plexiglas compartments with wire mesh bottom and von Frey filaments (2.44 to 4.31 (0.04–2.00 g), Stoelting, Wood Dale, IL, USA) were applied perpendicularly to the mid-hind paw and held for 4–6 s. Testing was performed daily for 3 days prior and

then daily after IS MBP(84-104) and MBPS injection. A positive response was noted if the paw was sharply withdrawn. The 50% probability of withdrawal threshold was determined by Dixon's up-down method (61). Data were analyzed using GraphPad Prism 4.04 (GraphPad, San Diego, CA, USA) by two-way analysis of variance (ANOVA) for repeated measures and Dunnett's post hoc test. $p \leq 0.05$ values were considered significant.

Drug delivery

The drugs were delivered at day 7 after IS MBP(84-104) injection. To allow intrathecal delivery, each mouse was placed under isoflurane anesthesia and was given a percutaneous intrathecal 5-μl bolus injection as previously described (62). Gabapentin (G117250, 100 mg/kg) was administered by i.p. injection in 0.9% NaCl (10 ml/kg). Xestospongin C (X2628, 1 nmol in 5 µl in 10% DMSO) or 10% DMSO (5 µl) were administered IT, followed by 10 μl of saline (0.9% NaCl) flush.

RNA-seq

Total RNA was extracted from mouse sciatic nerve (n = 12, pooled), L4/L5 DRG (n = 6, pooled), and L1-6 DSC (n = 6, pooled) ipsilateral to IS injection using TRI Reagent (Zymo Research, Irvine, CA, USA) and purified using Direct-zol RNA purification reagents (Zymo Research). Samples were treated with DNase I during purification. The RNA purity was estimated by measuring the OD260/280 ratio using a ND-1000 Spectrophotometer (Thermo Fisher Scientific). RNA integrity was confirmed using 2100 Bioanalyzer (Agilent Technologies, San Diego, CA, USA), and RNA samples with RIN $\geq$ 7.0 were processed further. Poly(A) RNA was isolated using the NEBNext® Poly(A) mRNA Magnetic Isolation Module and barcoded libraries were made using the NEBNext® Ultra II™ Directional RNA Library Prep Kit for Illumina® (New England Biolabs, Ipswich, MA). Libraries were pooled and single end sequenced (1X75) on the Illumina NextSeq 500 using the High output V2 kit (Illumina Inc., San Diego, CA, USA).

RNA-seq data processing

RNA-seq read data were processed using BaseSpace software (Illumina Inc.). Reads were aligned to the *Mus musculus* genome (mm10 assembly, RRID:SCR_002344) using STAR aligner (63) with default settings. Transcript and gene level expression was computed as transcripts per kilobase of TPM using Salmon software (64). Differential gene expression was determined using the Cufflinks package (65) on the Galaxy platform (66). Global DE analysis was conducted according to the previously established bioinformatic procedures (67–69). FC for each transcript with $p \leq 0.05$ was determined as ratios of TPM of IS MBP(84-104) or MBPS relative to the respective PBS control. Thresholds $\log_2$FC $>$ 0.585 (up-regulated) or $\log_2$FC $<$ -0.585 (down-regulated) relative to IS PBS were set to filter out insignificant changes in expression. Venn diagrams were plotted using R Limma package (70). Principal component analysis and hierarchical clustering were conducted using ClustVis engine (71). False discovery rate was controlled using Benjamini-Yekutieli p value correction (72). Canonical pathway analysis was performed using Ingenuity IPA (Qiagen Bioinformatics, Redwood City, CA, USA). p Values were calculated using right-tailed Fisher's exact test. Canonical pathways with $p \leq 0.05$ were considered for analysis. The activation status of the canonical pathways was predicted by calculating IPA Z-scores. Canonical pathways with $p \leq 0.05$ and Z-score $\geq$ 2.0 (or ≤ -2.0) were considered significantly activated (or inhibited). Gene list enrichment analysis to determine top GO Biological Processes (RRID:SCR_002811) was done using ToppGene Suite (43). GO biological processes with Bonferroni corrected $p \leq 0.05$ were considered for analysis. Gene and protein classification was conducted using PANTHER (73).

Data availability

The full transcriptomics data of the nerve, DRG, and spinal cord samples of all treatment groups of both sexes are available in a public repository (GEO ID GSE107159).

Author contributions—V. I. S., S. K. H., T. L. Y., A. V. C., and A. Y. S., conceptualization; A. V. C., V. I. S., and T. L. Y. data curation; A. V. C. and K. A. E. formal analysis; A. V. C. visualization; A. V. C., V. I. S., T. L. Y., and K. A. E. methodology; A. V. C. and V. I. S. writing-original draft; A. V. C., V. I. S., T. L. Y., and A. Y. S. writing-review and editing; S. K. H., K. A. E., J. D., A. G. R., M. A., and B. P. J. investigation; B. P. J. software; V. I. S., T. L. Y., and A. Y. S. resources; V. I. S., funding acquisition; V. I. S. project administration.

Funding and additional information—This work was supported by the National Institutes of Health Grant R01 DE022757 and National Institutes of Health Office of Research on Women's Health Administrative Supplement for Research on Sex/Gender Differences (to V. I. S., A. Y. S., and T. L. Y.), Department of Veterans Affairs Merit Award 5I01BX000638 (to V. I. S.), and University of California Academic Senate Research Grant RS283B (to V. I. S.). The content is solely the responsibility of the authors and does not necessarily represent the official views of the National Institutes of Health.

Conflict of interest—The authors declare that they have no conflicts of interest with the contents of this article.

Abbreviations—The abbreviations used are: DRG, dorsal root ganglia; MBP, myelin basic protein; PIP2, phosphatidylinositol 4,5-bisphosphate; SN, sciatic nerve; IS, injection into an intact sciatic nerve; DSC, dorsal spinal cord; TPM, transcript/million mapped reads; DE, differentially expressed; IPA, Ingenuity pathway analysis; VGCC, voltage-gated Ca^{2+} channel; IL, interleukin; DHCR7, 7-dehydrocholesterol reductase; PI3K, phosphoinositide 3-kinase; MAPK, mitogen-activated protein kinase; PKC, protein kinase C; TNFR, tumor necrosis factor; ESR, estrogen receptor; MIF, macrophage migration inhibitory factor; IP3, inositol trisphosphate receptor; ER, endoplasmic reticulum; IT, intrathecal; MBPS, MBP scramble; ANOVA, analysis of variance; NFAT, nuclear factor of activated T cells; GO, Gene ontology.

References

1. Treede, R. D., Jensen, T. S., Campbell, J. N., Cruccu, G., Dostrovsky, J. O., Griffin, J. W., Hansson, P., Hughes, R., Nurmikko, T., and Serra, J. (2008)

Neuropathic pain: redefinition and a grading system for clinical and research purposes. *Neurology* **70,** 1630–1635 CrossRef Medline
2. Nahin, R. L. (2015) Estimates of pain prevalence and severity in adults: United States, 2012. *J. Pain* **16,** 769–780 CrossRef Medline
3. Price, T. J., Basbaum, A. I., Bresnahan, J., Chambers, J. F., De Koninck, Y., Edwards, R. R., Ji, R. R., Katz, J., Kavelaars, A., Levine, J. D., Porter, L., Schechter, N., Sluka, K. A., Terman, G. W., Wager, T. D., *et al.* (2018) Transition to chronic pain: opportunities for novel therapeutics. *Nat. Rev. Neurosci.* **19,** 383–384 CrossRef
4. Boerner, K. E., Chambers, C. T., Gahagan, J., Keogh, E., Fillingim, R. B., and Mogil, J. S. (2018) Conceptual complexity of gender and its relevance to pain. *Pain* **159,** 2137–2141 CrossRef Medline
5. Unruh, A. M. (1996) Gender variations in clinical pain experience. *Pain* **65,** 123–167 CrossRef Medline
6. Fillingim, R. B., King, C. D., Ribeiro-Dasilva, M. C., Rahim-Williams, B., and Riley, J. L., 3rd (2009) Sex, gender, and pain: a review of recent clinical and experimental findings. *J. Pain* **10,** 447–485 CrossRef Medline
7. Greenspan, J. D., Craft, R. M., LeResche, L., Arendt-Nielsen, L., Berkley, K. J., Fillingim, R. B., Gold, M. S., Holdcroft, A., Lautenbacher, S., Mayer, E. A., Mogil, J. S., Murphy, A. Z., and Traub, R. J, Consensus Working Group of the Sex, G., SIG of the IASP. (2007) Studying sex and gender differences in pain and analgesia: a consensus report. *Pain* **132,** S26–S45 CrossRef
8. Sorge, R. E., and Totsch, S. K. (2017) Sex differences in pain. *J. Neurosci. Res.* **95,** 1271–1281 CrossRef Medline
9. Mogil, J. S. (2012) Sex differences in pain and pain inhibition: multiple explanations of a controversial phenomenon. *Nat. Rev. Neurosci.* **13,** 859–866 CrossRef Medline
10. Sorge, R. E., LaCroix-Fralish, M. L., Tuttle, A. H., Sotocinal, S. G., Austin, J. S., Ritchie, J., Chanda, M. L., Graham, A. C., Topham, L., Beggs, S., Salter, M. W., and Mogil, J. S. (2011) Spinal cord Toll-like receptor 4 mediates inflammatory and neuropathic hypersensitivity in male but not female mice. *J. Neurosci.* **31,** 15450–15454 CrossRef Medline
11. Sorge, R. E., Mapplebeck, J. C., Rosen, S., Beggs, S., Taves, S., Alexander, J. K., Martin, L. J., Austin, J. S., Sotocinal, S. G., Chen, D., Yang, M., Shi, X. Q., Huang, H., Pillon, N. J., Bilan, P. J., *et al.* (2015) Different immune cells mediate mechanical pain hypersensitivity in male and female mice. *Nat. Neurosci.* **18,** 1081–1083 CrossRef Medline
12. Lopes, D. M., Malek, N., Edye, M., Jager, S. B., McMurray, S., McMahon, S. B., and Denk, F. (2017) Sex differences in peripheral not central immune responses to pain-inducing injury. *Sci. Rep.* **7,** 16460 CrossRef Medline
13. Stephens, K. E., Chen, Z., Sivanesan, E., Raja, S. N., Linderoth, B., Taverna, S. D., and Guan, Y. (2018) RNA-seq of spinal cord from nerve-injured rats after spinal cord stimulation. *Mol. Pain* **14,** 1744806918817429 CrossRef Medline
14. Stokes, J. A., Cheung, J., Eddinger, K., Corr, M., and Yaksh, T. L. (2013) Toll-like receptor signaling adapter proteins govern spread of neuropathic pain and recovery following nerve injury in male mice. *J. Neuroinflammation* **10,** 148 CrossRef Medline
15. Moalem, G., Xu, K., and Yu, L. (2004) T lymphocytes play a role in neuropathic pain following peripheral nerve injury in rats. *Neuroscience* **129,** 767–777 CrossRef Medline
16. Kleinschnitz, C., Hofstetter, H. H., Meuth, S. G., Braeuninger, S., Sommer, C., and Stoll, G. (2006) T cell infiltration after chronic constriction injury of mouse sciatic nerve is associated with interleukin-17 expression. *Exp. Neurol.* **200,** 480–485 CrossRef Medline
17. Costigan, M., Moss, A., Latremoliere, A., Johnston, C., Verma-Gandhu, M., Herbert, T. A., Barrett, L., Brenner, G. J., Vardeh, D., Woolf, C. J., and Fitzgerald, M. (2009) T-cell infiltration and signaling in the adult dorsal spinal cord is a major contributor to neuropathic pain-like hypersensitivity. *J. Neurosci.* **29,** 14415–14422 CrossRef Medline
18. Draleau, K., Maddula, S., Slaiby, A., Nutile-McMenemy, N., De Leo, J., and Cao, L. (2014) Phenotypic identification of spinal cord-infiltrating CD4 T lymphocytes in a murine model of neuropathic pain. *J. Pain Relief* **3,** 003 CrossRef Medline
19. Rosen, S. F., Ham, B., Drouin, S., Boachie, N., Chabot-Dore, A. J., Austin, J. S., Diatchenko, L., and Mogil, J. S. (2017) T-cell mediation of pregnancy analgesia affecting chronic pain in mice. *J. Neurosci.* **37,** 9819–9827 CrossRef Medline
20. Taveggia, C., Feltri, M. L., and Wrabetz, L. (2010) Signals to promote myelin formation and repair. *Nat. Rev. Neurol.* **6,** 276–287 CrossRef Medline
21. Boggs, J. M. (2006) Myelin basic protein: a multifunctional protein. *Cell Mol. Life Sci.* **63,** 1945–1961 CrossRef Medline
22. Harauz, G., Ladizhansky, V., and Boggs, J. M. (2009) Structural polymorphism and multifunctionality of myelin basic protein. *Biochemistry* **48,** 8094–8104 CrossRef Medline
23. Nawaz, S., Kippert, A., Saab, A. S., Werner, H. B., Lang, T., Nave, K. A., and Simons, M. (2009) Phosphatidylinositol 4,5-bisphosphate-dependent interaction of myelin basic protein with the plasma membrane in oligodendroglial cells and its rapid perturbation by elevated calcium. *J. Neurosci.* **29,** 4794–4807 CrossRef Medline
24. Devor, M. (2009) Ectopic discharge in Abeta afferents as a source of neuropathic pain. *Exp. Brain Res.* **196,** 115–128 CrossRef Medline
25. Henry, M. A., Luo, S., Foley, B. D., Rzasa, R. S., Johnson, L. R., and Levinson, S. R. (2009) Sodium channel expression and localization at demyelinated sites in painful human dental pulp. *J. Pain* **10,** 750–758 CrossRef Medline
26. Kobayashi, H., Chattopadhyay, S., Kato, K., Dolkas, J., Kikuchi, S., Myers, R. R., and Shubayev, V. I. (2008) MMPs initiate Schwann cell-mediated MBP degradation and mechanical nociception after nerve damage. *Mol. Cell. Neurosci.* **39,** 619–627 CrossRef Medline
27. Kadlubowski, M., and Hughes, R. A. (1979) Identification of the neuritogen for experimental allergic neuritis. *Nature* **277,** 140–141 CrossRef Medline
28. Hong, S., Remacle, A. G., Shiryaev, S. A., Choi, W., Hullugundi, S. K., Dolkas, J., Angert, M., Nishihara, T., Yaksh, T. L., Strongin, A. Y., and Shubayev, V. I. (2017) Reciprocal relationship between membrane type 1 matrix metalloproteinase and the algesic peptides of myelin basic protein contributes to chronic neuropathic pain. *Brain Behav. Immun.* **60,** 282–292 CrossRef Medline
29. Liu, H., Shiryaev, S. A., Chernov, A. V., Kim, Y., Shubayev, I., Remacle, A. G., Baranovskaya, S., Golubkov, V. S., Strongin, A. Y., and Shubayev, V. I. (2012) Immunodominant fragments of myelin basic protein initiate T cell-dependent pain. *J. Neuroinflammation* **9,** 119 CrossRef
30. Chernov, A. V., Remacle, A. G., Hullugundi, S. K., Cieplak, P., Angert, M., Dolkas, J., Shubayev, V. I., and Strongin, A. Y. (2018) Amino acid sequence conservation of the algesic fragment of myelin basic protein is required for its interaction with CDK5 and function in pain. *FEBS J.* **285,** 3485–3502 CrossRef Medline
31. Remacle, A. G., Dolkas, J., Angert, M., Hullugundi, S. K., Chernov, A. V., Jones, R. C. W., 3rd, Shubayev, V. I., and Strongin, A. Y. (2018) A sensitive and selective ELISA methodology quantifies a demyelination marker in experimental and clinical samples. *J. Immunol. Methods* **455,** 80–87 CrossRef Medline
32. Ko, J. S., Eddinger, K. A., Angert, M., Chernov, A. V., Dolkas, J., Strongin, A. Y., Yaksh, T. L., and Shubayev, V. I. (2016) Spinal activity of interleukin 6 mediates myelin basic protein-induced allodynia. *Brain Behav. Immun.* **56,** 378–389 CrossRef Medline
33. Shubayev, V. I., Strongin, A. Y., and Yaksh, T. L. (2018) Structural homology of myelin basic protein and muscarinic acetylcholine receptor: Significance in the pathogenesis of complex regional pain syndrome. *Mol. Pain* **14,** 1744806918815005 CrossRef Medline
34. Remacle, A. G., Hullugundi, S. K., Dolkas, J., Angert, M., Cieplak, P., Scott, D., Chernov, A. V., Shubayev, V. I., and Strongin, A. Y. (2018) Interaction of the cryptic fragment of myelin basic protein with mitochondrial voltage-dependent anion-selective channel-1 affects cell energy metabolism. *Biochem. J.* **475,** 2355–2376 CrossRef Medline
35. Shubayev, V. I., Strongin, A. Y., and Yaksh, T. L. (2016) Role of myelin auto-antigens in pain: a female connection. *Neural Regen. Res.* **11,** 890–891 CrossRef Medline
36. Hammer, P., Banck, M. S., Amberg, R., Wang, C., Petznick, G., Luo, S., Khrebtukova, I., Schroth, G. P., Beyerlein, P., and Beutler, A. S. (2010) mRNA-seq with agnostic splice site discovery for nervous system transcriptomics tested in chronic pain. *Genome Res.* **20,** 847–860 CrossRef Medline

37. Kim, Y., Remacle, A. G., Chernov, A. V., Liu, H., Shubayev, I., Lai, C., Dolkas, J., Shiryaev, S. A., Golubkov, V. S., Mizisin, A. P., Strongin, A. Y., and Shubayev, V. I. (2012) The MMP-9/TIMP-1 axis controls the status of differentiation and function of myelin-forming Schwann cells in nerve regeneration. *PLoS ONE* **7,** e33664 CrossRef Medline
38. Raju, H. B., Tsinoremas, N. F., and Capobianco, E. (2016) Emerging putative associations between non-coding RNAs and protein-coding genes in neuropathic pain: added value from reusing microarray data. *Front. Neurol.* **7,** 168 CrossRef Medline
39. Wu, S., Marie Lutz, B., Miao, X., Liang, L., Mo, K., Chang, Y. J., Du, P., Soteropoulos, P., Tian, B., Kaufman, A. G., Bekker, A., Hu, Y., and Tao, Y. X. (2016) Dorsal root ganglion transcriptome analysis following peripheral nerve injury in mice. *Mol. Pain* **12,** 174480691662904 CrossRef
40. Hirai, T., Mulpuri, Y., Cheng, Y., Xia, Z., Li, W., Ruangsri, S., Spigelman, I., and Nishimura, I. (2017) Aberrant plasticity of peripheral sensory axons in a painful neuropathy. *Sci. Rep.* **7,** 3407 CrossRef Medline
41. Cobos, E. J., Nickerson, C. A., Gao, F., Chandran, V., Bravo-Caparrós, I., González-Cano, R., Riva, P., Andrews, N. A., Latremoliere, A., Seehus, C. R., Perazzoli, G., Nieto, F. R., Joller, N., Painter, M. W., Ma, C. H. E., *et al.* (2018) Mechanistic differences in neuropathic pain modalities revealed by correlating behavior with global expression profiling. *Cell Rep.* **22,** 1301–1312 CrossRef Medline
42. Chernov, A. V., Dolkas, J., Hoang, K., Angert, M., Srikrishna, G., Vogl, T., Baranovskaya, S., Strongin, A. Y., and Shubayev, V. I. (2015) The calcium-binding proteins S100A8 and S100A9 initiate the early inflammatory program in injured peripheral nerves. *J. Biol. Chem.* **290,** 11771–11784 CrossRef Medline
43. Chen, J., Bardes, E. E., Aronow, B. J., and Jegga, A. G. (2009) ToppGene Suite for gene list enrichment analysis and candidate gene prioritization. *Nucleic Acids Res.* **37,** W305–311 CrossRef Medline
44. Corona, J. C., and Duchen, M. R. (2016) PPARγ as a therapeutic target to rescue mitochondrial function in neurological disease. *Free Radic. Biol. Med.* **100,** 153–163 CrossRef Medline
45. Prato, V., Taberner, F. J., Hockley, J. R. F., Callejo, G., Arcourt, A., Tazir, B., Hammer, L., Schad, P., Heppenstall, P. A., Smith, E. S., and Lechner, S. G. (2017) Functional and molecular characterization of mechanoinsensitive "silent" nociceptors. *Cell Rep.* **21,** 3102–3115 CrossRef Medline
46. Held, R. G., and Kaeser, P. S. (2018) ELKS active zone proteins as multitasking scaffolds for secretion. *Open Biol.* **8,** 170258 CrossRef
47. Oka, T., Sato, K., Hori, M., Ozaki, H., and Karaki, H. (2002) Xestospongin C, a novel blocker of IP3 receptor, attenuates the increase in cytosolic calcium level and degranulation that is induced by antigen in RBL-2H3 mast cells. *Br. J. Pharmacol.* **135,** 1959–1966 CrossRef Medline
48. Khomula, E. V., Ferrari, L. F., Araldi, D., and Levine, J. D. (2017) Sexual dimorphism in a reciprocal interaction of ryanodine and IP3 receptors in the induction of hyperalgesic priming. *J. Neurosci.* **37,** 2032–2044 CrossRef Medline
49. Blackburn-Munro, G., and Erichsen, H. K. (2005) Antiepileptics and the treatment of neuropathic pain: evidence from animal models. *Curr. Pharm. Design* **11,** 2961–2976 CrossRef Medline
50. Remacle, A. G., Hullugundi, S. K., Dolkas, J., Angert, M., Chernov, A. V., Strongin, A. Y., and Shubayev, V. I. (2018) Acute- and late-phase matrix metalloproteinase (MMP)-9 activity is comparable in female and male rats after peripheral nerve injury. *J. Neuroinflammation* **15,** 89 CrossRef Medline
51. Myers, R. R., Campana, W. M., and Shubayev, V. I. (2006) The role of neuroinflammation in neuropathic pain: mechanisms and therapeutic targets. *Drug Discov. Today* **11,** 8–20 CrossRef Medline
52. Scholz, J., and Woolf, C. J. (2007) The neuropathic pain triad: neurons, immune cells and glia. *Nat. Neurosci.* **10,** 1361–1368 CrossRef Medline
53. Demarest, T. G., and McCarthy, M. M. (2015) Sex differences in mitochondrial (dys)function: Implications for neuroprotection. *J. Bioenerg. Biomembr.* **47,** 173–188 CrossRef Medline
54. Castonguay, A., and Robitaille, R. (2002) Xestospongin C is a potent inhibitor of SERCA at a vertebrate synapse. *Cell Calcium* **32,** 39–47 CrossRef
55. Solovyova, N., Fernyhough, P., Glazner, G., and Verkhratsky, A. (2002) Xestospongin C empties the ER calcium store but does not inhibit InsP3-induced Ca^{2+} release in cultured dorsal root ganglia neurones. *Cell Calcium* **32,** 49–52 CrossRef
56. Perera, C. J., Duffy, S. S., Lees, J. G., Kim, C. F., Cameron, B., Apostolopoulos, V., and Moalem-Taylor, G. (2015) Active immunization with myelin-derived altered peptide ligand reduces mechanical pain hypersensitivity following peripheral nerve injury. *J. Neuroinflammation* **12,** 28 CrossRef Medline
57. Devor, M. (1999) Unexplained peculiarities of the dorsal root ganglion. *Pain* **6,** S27–S35 CrossRef
58. Zagni, E., Simoni, L., and Colombo, D. (2016) Sex and gender differences in central nervous system-related disorders. *Neurosci. J.* **2016,** 2827090 CrossRef Medline
59. Voskuhl, R. (2011) Sex differences in autoimmune diseases. *Biol. Sex Differ.* **2,** 1 CrossRef Medline
60. Whitacre, C. C., Reingold, S. C., and O'Looney, P. A. (1999) A gender gap in autoimmunity. *Science* **283,** 1277–1278 CrossRef Medline
61. Chaplan, S. R., Bach, F. W., Pogrel, J. W., Chung, J. M., and Yaksh, T. L. (1994) Quantitative assessment of tactile allodynia in the rat paw. *J. Neurosci. Methods* **53,** 55–63 CrossRef Medline
62. Hylden, J. L., and Wilcox, G. L. (1980) Intrathecal morphine in mice: a new technique. *Eur. J. Pharmacol.* **67,** 313–316 CrossRef Medline
63. Dobin, A., Davis, C. A., Schlesinger, F., Drenkow, J., Zaleski, C., Jha, S., Batut, P., Chaisson, M., and Gingeras, T. R. (2013) STAR: ultrafast universal RNA-seq aligner. *Bioinformatics* **29,** 15–21 CrossRef Medline
64. Patro, R., Duggal, G., Love, M. I., Irizarry, R. A., and Kingsford, C. (2017) Salmon provides fast and bias-aware quantification of transcript expression. *Nat. Methods* **14,** 417–419 CrossRef Medline
65. Trapnell, C., Williams, B. A., Pertea, G., Mortazavi, A., Kwan, G., van Baren, M. J., Salzberg, S. L., Wold, B. J., and Pachter, L. (2010) Transcript assembly and quantification by RNA-Seq reveals unannotated transcripts and isoform switching during cell differentiation. *Nat. Biotechnol.* **28,** 511–515 CrossRef Medline
66. Afgan, E., Baker, D., van den Beek, M., Blankenberg, D., Bouvier, D., Čech, M., Chilton, J., Clements, D., Coraor, N., Eberhard, C., Grüning, B., Guerler, A., Hillman-Jackson, J., Von Kuster, G., Rasche, E., *et al.* (2016) The Galaxy platform for accessible, reproducible and collaborative biomedical analyses: 2016 update. *Nucleic Acids Res* **44,** W3–W10 CrossRef Medline
67. Chen, Y., Lun, A. T., and Smyth, G. K. (2016) From reads to genes to pathways: differential expression analysis of RNA-Seq experiments using Rsubread and the edgeR quasi-likelihood pipeline. *F1000Res.* **5,** 1438 CrossRef Medline
68. Soneson, C., Love, M. I., and Robinson, M. D. (2015) Differential analyses for RNA-seq: transcript-level estimates improve gene-level inferences. *F1000Res.* **4,** 1521 CrossRef Medline
69. Love, M. I., Anders, S., Kim, V., and Huber, W. (2015) RNA-Seq workflow: gene-level exploratory analysis and differential expression. *F1000Res.* **4,** 1070 CrossRef Medline
70. Law, C. W., Alhamdoosh, M., Su, S., Smyth, G. K., and Ritchie, M. E. (2016) RNA-seq analysis is easy as 1-2-3 with limma, Glimma and edgeR. *F1000Res.* **5,** 1408 CrossRef
71. Metsalu, T., and Vilo, J. (2015) ClustVis: a web tool for visualizing clustering of multivariate data using principal component analysis and heatmap. *Nucleic Acids Res* **43,** W566–W570 CrossRef Medline
72. Reiner, A., Yekutieli, D., and Benjamini, Y. (2003) Identifying differentially expressed genes using false discovery rate controlling procedures. *Bioinformatics* **19,** 368–375 CrossRef Medline
73. Mi, H., Muruganujan, A., and Thomas, P. D. (2013) PANTHER in 2013: modeling the evolution of gene function, and other gene attributes, in the context of phylogenetic trees. *Nucleic Acids Res.* **41,** D377–D386 CrossRef Medline